JOURNAL OF COMPUTATIONAL PHYSICS 40, 478–490 (1981)

Continuous Transformation Computation of Boundary Layer Equations between Similarity Regimes

ROLAND HUNT AND GRAHAM WILKS

Department of Mathematics, University of Strathclyde, Glasgow, Scotland

Received March 31, 1980

Consideration is given to the computation of boundary layer flows displaying evolution between similarity regimes. A continuous transformation is introduced which reflects the associated evolution. When applied in conjunction with recent developments involving extrapolation on crude nets an efficient, accurate and straightforward algorithm ensues.

1. INTRODUCTION

In investigations of non-similar boundary layer flows is has long been customary to exploit a knowledge of "near" similarity over a coordinate range to transform the governing boundary layer equations into a form amenable to numerical computation or series expansion analysis. For instance, the similarity solutions of Blasius and Falkner–Skan frequently provide the basis for similarity transformations of the boundary layer equations when considering regular perturbations of flows about sharp or blunt leading edges. A particular class of problem concerns flows involving the evolution, with respect to a characterising coordinate (either time-like or space-like), from one similarity regime to another. Investigation of such flows typically involves regular and inverse coordinate expansion about the asymptotically valid similarity solution appropriate to each of the unperturbed regimes. To substantiate the validity of the series solutions it is usual to undertake a full numerical integration of the governing equations. This has, in the past, been achieved by initiating the integration in the context of one set of transformed variables and its associated equations up to a coordinate location where their suitability starts to become questionable. At this stage, usually at a convenient coordinate location if the problem has been well formulated, the algorithm continues via a switch to the set of equations associated with the transformed variables appropriate to the final similarity regime. In this paper we indicate that the somewhat unwieldy switch between two sets of governing equations may be avoided by the introduction of a continuous transformation, in the characterising coordinate, reflecting the prior knowledge of the respective similarity regimes.

0021-9991/81/040478–13$02.00/0

2. Illustrative Problems

To demonstrate the continuous transformation computation we have chosen to re-examine two mixed convection boundary layer problems which have appeared in the literature. They are concerned with the effect of buoyancy forces on the flow of a uniform stream over a semi-infinite vertical plate whose leading edge is aligned horizontally. Accelerating buoyancy forces result from the application of (a) the uniform temperature [1], (b) the uniform heat flux [2] boundary constraint at the plate. Each flow provides an ideal illustration of the evolution between two similarity states. Near the leading edge there is little opportunity for heat from the plate to be assimilated by the fluid and the boundary layer is formed mainly by the retardation of the free stream by viscosity. Away from the leading edge, however, buoyancy forces become increasingly important until far downstream the flow will be predominantly one of free convection perturbed by the presence of the free stream. Each flow can be characterised by a non-dimensional coordinate reflecting the local relative importance of viscous and buoyancy forces. Accordingly an evolution in the appropriate coordinate between the similarity states of Blasius and (a) Ostrach [3] and (b) Sparrow and Gregg [4] characterises each problem.

3. Equations and Transformations

In the usual notation the governing boundary layer equations representing conservation of mass, momentum and energy, respectively, are

$$\frac{\partial u}{\partial x}+\frac{\partial v}{\partial y}=0, \tag{1}$$

$$u\frac{\partial u}{\partial x}+v\frac{\partial u}{\partial y}=g\beta(T-T_0)+\nu\frac{\partial^2 u}{\partial y^2}, \tag{2}$$

$$u\frac{\partial T}{\partial x}+v\frac{\partial T}{\partial y}=\kappa\frac{\partial^2 T}{\partial y^2} \tag{3}$$

to be solved subject to the boundary conditions

$$u=v=0, \quad \begin{matrix}\text{(a)}\quad T=T_1\\ \text{(b)}\quad \dfrac{\partial T}{\partial y}=\dfrac{-q}{k}\end{matrix} \quad \text{on } y=0 \tag{4}$$

$$u\to U,\ T\to T_0 \text{ as } y\to\infty.$$

(a) *Uniform Temperature*

The characteristic non-dimensional coordinate employed by Merkin for this case is

$$\xi_M = \frac{Gr_x}{Re_x} = \frac{g\beta(T_1 - T_0)x}{U^2}, \tag{5}$$

where Gr_x and Re_x are local Grashof and Reynolds numbers based on the distance from the leading edge.

Transformations appropriate to the leading edge and downstream regimes are respectively

Blasius	Ostrach
$\psi = (2\nu U x)^{1/2} f(\xi_M, \eta),$	$\psi = 4\nu C x^{3/4} \bar{f}(\xi_M, \bar{\eta}),$
$T - T_0 = (T_1 - T_0)\,\theta(\xi_M, \eta),$	$T - T_0 = (T_1 - T_0)\,\bar{\theta}(\xi_M, \bar{\eta}),$
$\eta = y\left(\frac{U}{2\nu x}\right)^{1/2},$	$\bar{\eta} = \frac{Cy}{x^{1/4}};\ C = \left(\frac{g\beta(T_1 - T_0)}{4\nu^2}\right)^{1/4}.$

(6)

leading to the two distinct sets of equations which provided the orginal basis for the computation algorithm

$$\frac{\partial^3 f}{\partial \eta^3} + f\frac{\partial^2 f}{\partial \eta^2} + 2\xi_M\theta = 2\xi_M\left(\frac{\partial^2 f}{\partial \xi_M \partial \eta}\frac{\partial f}{\partial \eta} - \frac{\partial^2 f}{\partial \eta^2}\frac{\partial f}{\partial \xi_M}\right)$$

$$\frac{1}{\sigma}\frac{\partial^2 \theta}{\partial \eta^2} + f\frac{\partial \theta}{\partial \eta} = 2\xi_M\left(\frac{\partial f}{\partial \eta}\frac{\partial \theta}{\partial \xi_M} - \frac{\partial f}{\partial \xi_M}\frac{\partial \theta}{\partial \eta}\right)$$

$$f = \frac{\partial f}{\partial \eta} = 0,\ \theta = 1 \text{ as } \eta = 0$$

$$\frac{\partial \theta}{\partial \eta} = 1,\ \theta \to 0 \text{ as } \eta \to \infty$$

$$\frac{\partial^3 \bar{f}}{\partial \bar{\eta}^3} + 3\bar{f}\frac{\theta^2 \bar{f}}{\partial \bar{\eta}^2} - 2\left(\frac{\partial \bar{f}}{\partial \bar{\eta}}\right)^2 + \bar{\theta} = 4\xi_M\left(\frac{\partial^2 \bar{f}}{\partial \xi_M \partial \bar{\eta}}\frac{\partial \bar{f}}{\partial \bar{\eta}} - \frac{\partial^2 \bar{f}}{\partial \bar{\eta}^2}\frac{\partial \bar{f}}{\partial \xi_M}\right)$$

$$\frac{1}{\sigma}\frac{\partial^2 \bar{\theta}}{\partial \bar{\eta}^2} + 3\bar{f}\frac{\partial \bar{\theta}}{\partial \bar{\eta}} = 4\xi_M\left(\frac{\partial \bar{f}}{\partial \bar{\eta}}\frac{\partial \bar{\theta}}{\partial \xi_M} - \frac{\partial \bar{f}}{\partial \xi_M}\frac{\partial \bar{\theta}}{\partial \bar{\eta}}\right)$$

$$\bar{f} = \frac{\partial \bar{f}}{\partial \bar{\eta}} = 0,\ \bar{\theta} = 1 \text{ on } \bar{\eta} = 0$$

$$\frac{\partial \bar{\theta}}{\partial \bar{\eta}} \to 2\xi_M^{-1/2},\ \bar{\theta} \to 0 \text{ as } \bar{\eta} \to \infty \tag{7}$$

($\sigma \equiv$ Prandtl Number).

Significantly

$$\eta = \xi_M^{-1/4}\bar{\eta};\qquad f = 2\xi_M^{1/4}\bar{f};\qquad \theta = \bar{\theta};\qquad \frac{\partial f}{\partial \eta} = 2\xi_M^{1/2}\frac{\partial \bar{f}}{\partial \bar{\eta}} \tag{8}$$

and accordingly a convenient switch from one system to the other at $\xi_M = 1$ facilitates successful integration over all ξ_M. Clearly the separate transformations are useful for pursuing perturbation analyses in the distinct regimes. However, when it comes to full numerical integration the distinction is not entirely a natural one, witness the evolution of velocity profiles with respect to the boundary condition away from the plate. Is it possible to formulate the transformations in a way which more naturally reflects the evolution between the two basic similarity regimes and simultaneously avoids the unwieldy switch necessitated in the above algorithm?

Since integration must of necessity be initiated in the Blasius regime we examine the possibility of continuous transformations

$$\psi = (2\nu U x)^{1/2} r(\xi_M) \tilde{f}(\xi_M, \tilde{\eta}); \quad T - T_0 = (T_1 - T_0)\, s(\xi_M)\, \tilde{\theta}(\xi_M, \tilde{\eta}), \tag{9}$$

$$\eta = y \left(\frac{U}{2\nu x} \right)^{1/2} t(\xi_M),$$

where $r(\xi_M)$, $s(\xi_M)$ and $t(\xi_M)$ are to be chosen to allow a smooth transition towards the pure free convection regime.

In general transformations (9) in (1)–(3) lead to

$$\frac{\partial^3 \tilde{f}}{\partial \tilde{\eta}^3} + \tilde{f} \frac{\partial^2 \tilde{f}}{\partial \tilde{\eta}^2} \left\{ \frac{r}{t} + 2\xi_M \frac{r'}{t} \right\} - \left(\frac{\partial \tilde{f}}{\partial \tilde{\eta}} \right)^2 \left\{ 2\xi_M \frac{r'}{t} + 2\xi_M \frac{rt'}{t^2} \right\}$$
$$+ 2\xi_M \frac{s\tilde{\theta}}{t^3 r} + 2\xi_M \frac{r}{t} \left\{ \frac{\partial^2 \tilde{f}}{\partial \tilde{\eta}^2} \frac{\partial \tilde{f}}{\partial \xi_M} - \frac{\partial \tilde{f}}{\partial \tilde{\eta}} \frac{\partial^2 \tilde{f}}{\partial \xi_M \partial \tilde{\eta}} \right\} = 0, \tag{10}$$

$$\frac{1}{\sigma} \frac{\partial^2 \tilde{\theta}}{\partial \tilde{\eta}^2} + \tilde{f} \frac{\partial \tilde{\theta}}{\partial \tilde{\eta}} \left\{ \frac{r}{t} + 2\xi_M \frac{r'}{t} \right\}$$
$$+ 2\xi_M \frac{r}{t} \left\{ \frac{\partial \tilde{\theta}}{\partial \tilde{\eta}} \frac{\partial \tilde{f}}{\partial \xi_M} - \frac{\partial \tilde{\theta}}{\partial \xi_M} \frac{\partial \tilde{f}}{\partial \tilde{\eta}} \right\} = 0 \qquad \left(' \equiv \frac{d}{d\xi_M} \right).$$

Without loss of generality we can prescribe $r(0) = s(0) = t(0) = 1$ and together with (8) one is led to the conclusion that choosing

$$r(\xi_M) = t(\xi_M) = (1 + \xi_M)^{1/4}; \qquad s(\xi_M) = 1 \tag{11}$$

will provide the basis for the required continuous transformation. Accordingly we anticipate that the single system of equations

$$\frac{\partial^3 \tilde{f}}{\partial \tilde{\eta}^3} + \frac{(4 + 6\xi_M)}{4(1 + \xi_M)} \tilde{f} \frac{\partial^2 \tilde{f}}{\partial \tilde{\eta}^2} - \left(\frac{\xi_M}{1 + \xi_M} \right) \left(\frac{\partial \tilde{f}}{\partial \tilde{\eta}} \right)^2 + \frac{2\xi_M \tilde{\theta}}{1 + \xi_M}$$
$$= 2\xi_M \left\{ \frac{\partial^2 \tilde{f}}{\partial \xi_M \partial \tilde{\eta}} \frac{\partial \tilde{f}}{\partial \tilde{\eta}} - \frac{\partial^2 \tilde{f}}{\partial \tilde{\eta}^2} \frac{\partial \tilde{f}}{\partial \xi_M} \right\}, \tag{12}$$

$$\frac{1}{\sigma} \frac{\partial^2 \tilde{\theta}}{\partial \tilde{\eta}^2} + \frac{(4 + 6\xi_M)}{4(1 + \xi_M)} \tilde{f} \frac{\partial \tilde{\theta}}{\partial \tilde{\eta}} = 2\xi_M \left\{ \frac{\partial \tilde{f}}{\partial \tilde{\eta}} \frac{\partial \tilde{\theta}}{\partial \xi_M} - \frac{\partial \tilde{f}}{\partial \xi_M} \frac{\partial \tilde{\theta}}{\partial \tilde{\eta}} \right\}$$

may be utilised for the complete numerical integration of the boundary layer flow between Blasius and Ostrach similarity regimes. In particular we note that the non-dimensional velocity unity at infinity implies

$$\frac{\partial \tilde{f}}{\partial \tilde{\eta}} = \frac{1}{r(\xi_M)t(\xi_M)} = \frac{1}{(1+\xi_M)^{1/2}} \qquad \text{as} \quad \tilde{\eta} \to \infty. \tag{13}$$

The velocity profiles may thus be expected to evolve continuously between their pure forced and pure free convection asymptotes.

(b) *Uniform Heat Flux*

The characteristic non-dimensional coordinate for this case was introduced by Wilks as

$$\xi_w = \left(\frac{2^3 Gr_x^2 Nu_x^2}{5^2 Re_x}\right)^{1/3} = \left(\frac{2^3 g^2 \beta^2 q^2 \nu}{5^2 k^2 U^5}\right)^{1/3} x, \tag{14}$$

where Nu_x is the local Nusselt number based on x.

The appropriate transformations are

Blasius	Sparrow and Gregg
$\psi = (2\nu U x)^{1/2} f(\xi_w),$	$\psi = C_2 x^{4/5} \hat{f}(\xi_w, \hat{\eta}),$
$T - T_0 = -\frac{q}{k}\left(\frac{2\nu x}{U}\right)^{1/2} \theta,$	$T - T_0 = \frac{-qx^{1/5}}{kC_3} \hat{\theta}(\xi_w, \hat{\eta}),$
$\eta = y\left(\frac{U}{2\nu x}\right)^{1/2},$	$\hat{\eta} = \frac{C_3 y}{x^{1/5}},$
	$C_2 = \left(\frac{2^4 5^4 g\beta q \nu^3}{k}\right)^{1/5}; \quad C_3 = \left(\frac{g\beta q}{2.5 \cdot k\nu^2}\right)^{1/5}$

(15)

and the distinct sets of equations are

$$\frac{\partial^3 f}{\partial \eta^3} + f\frac{\partial^2 f}{\partial \eta^2} - 5\xi_w^{3/2}\theta = 2\xi_w\left\{\frac{\partial^2 f}{\partial \xi_w \partial \eta}\frac{\partial f}{\partial \eta} - \frac{\partial^2 f}{\partial \eta^2}\frac{\partial f}{\partial \xi_w}\right\}$$

$$\frac{1}{\sigma}\frac{\partial^2 \theta}{\partial \eta^2} + f\frac{\partial \theta}{\partial \eta} - \theta\frac{\partial f}{\partial \eta} = 2\xi_w\left\{\frac{\partial f}{\partial \eta}\frac{\partial \theta}{\partial \xi_w} - \frac{\partial f}{\partial \xi_w}\frac{\partial \theta}{\partial \eta}\right\}$$

$$\frac{\partial^3 \hat{f}}{\partial \hat{\eta}^3} + 8\hat{f}\frac{\partial^2 \hat{f}}{\partial \hat{\eta}^2} - 6\left(\frac{\partial \hat{f}}{\partial \hat{\eta}}\right)^2 - \hat{\theta} = 10\xi_w\left\{\frac{\partial^2 \hat{f}}{\partial \hat{\eta} \partial \xi_w}\frac{\partial \hat{f}}{\partial \hat{\eta}} - \frac{\partial^2 \hat{f}}{\partial \hat{\eta}^2}\frac{\partial \hat{f}}{\partial \xi_w}\right\}$$

$$\frac{1}{\sigma}\frac{\partial^2 \hat{\theta}}{\partial \hat{\eta}^2} + 8\hat{f}\frac{\partial \hat{\theta}}{\partial \hat{\eta}} - 2\hat{\theta}\frac{\partial \hat{f}}{\partial \hat{\eta}} = 10\xi_w\left\{\frac{\partial \hat{f}}{\partial \hat{\eta}}\frac{\partial \hat{\theta}}{\partial \xi_w} - \frac{\partial \hat{f}}{\partial \xi_w}\frac{\partial \hat{\theta}}{\partial \hat{\eta}}\right\}$$

$$f=\frac{\partial f}{\partial \eta}=0;\ \frac{\partial \theta}{\partial \eta}=1 \text{ on } \eta=0 \qquad \hat{f}=\frac{\partial \hat{f}}{\partial \hat{\eta}}=0;\ \frac{\partial \hat{\theta}}{\partial \hat{\eta}}=1 \text{ on } \hat{\eta}=0$$

$$\frac{\partial f}{\partial \eta}\to 1;\ \theta\to 0 \text{ as } \eta\to\infty \qquad \frac{\partial \hat{f}}{\partial \hat{\eta}}\to \frac{1}{5}\xi_{\mathrm{w}}^{-3/5};\ \hat{\theta}\to 0 \text{ as } \hat{\eta}\to\infty. \tag{16}$$

The counterparts of (8) now read

$$\eta=\xi_{\mathrm{w}}^{-3/10}\hat{\eta};\qquad f=5\xi_{\mathrm{w}}^{3/10}\hat{f};\qquad \theta=\xi_{\mathrm{w}}^{-3/10}\hat{\theta};\qquad \frac{\partial f}{\partial \eta}=5\xi^{3/5}\frac{\partial \hat{f}}{\partial \hat{\eta}}. \tag{17}$$

Invoking the continuous transformation

$$\psi=(2\nu Ux)^{1/2}r(\xi_{\mathrm{w}})\tilde{f}(\xi_{\mathrm{w}},\tilde{\eta});\qquad T-T_0=\frac{-q}{k}\left(\frac{2\nu x}{U}\right)^{1/2}s(\xi_{\mathrm{w}})\,\tilde{\theta}(\xi_{\mathrm{w}},\tilde{\eta}),$$
$$\tilde{\eta}=y\left(\frac{U}{2\nu x}\right)^{1/2}t(\xi_{\mathrm{w}}) \tag{18}$$

yields

$$\begin{aligned}
&\frac{\partial^3\tilde{f}}{\partial\tilde{\eta}^3}+\tilde{f}\frac{\partial^2\tilde{f}}{\partial\tilde{\eta}^2}\left\{\frac{r}{t}+2\xi_{\mathrm{w}}\frac{r'}{t}\right\}-\left(\frac{\partial\tilde{f}}{\partial\tilde{\eta}}\right)^2\left\{\frac{2\xi_{\mathrm{w}}r'}{t}+2\xi_{\mathrm{w}}\frac{rt'}{t^2}\right\}-\frac{5\xi_{\mathrm{w}}^{3/2}s\tilde{\theta}}{t^3r}\\
&\quad=2\xi_{\mathrm{w}}\frac{r}{t}\left\{\frac{\partial^2\tilde{f}}{\partial\tilde{\eta}\,\partial\xi_{\mathrm{w}}}\frac{\partial\tilde{f}}{\partial\tilde{\eta}}-\frac{\partial^2\tilde{f}}{\partial\tilde{\eta}^2}\frac{\partial\tilde{f}}{\partial\xi_{\mathrm{w}}}\right\},\\
&\frac{1}{\sigma}\frac{\partial^2\tilde{\theta}}{\partial\tilde{\eta}^2}+\tilde{f}\frac{\partial\tilde{\theta}}{\partial\tilde{\eta}}\left\{\frac{r}{t}+2\xi_{\mathrm{w}}\frac{r'}{t}\right\}-\tilde{\theta}\frac{\partial\tilde{f}}{\partial\tilde{\eta}}\left\{\frac{r}{t}+\frac{2\xi_{\mathrm{w}}r\cdot s'}{t\cdot s}\right\}\\
&\quad=2\xi_{\mathrm{w}}\frac{r}{t}\left\{\frac{\partial\tilde{f}}{\partial\tilde{\eta}}\frac{\partial\tilde{\theta}}{\partial\xi_{\mathrm{w}}}-\frac{\partial\tilde{f}}{\partial\xi_{\mathrm{w}}}\frac{\partial\tilde{\theta}}{\partial\tilde{\eta}}\right\}.
\end{aligned} \tag{19}$$

Similar arguments as for the case (a) lead to the choice

$$r(\xi_{\mathrm{w}})=(1+\xi_{\mathrm{w}})^{3/10},\qquad t(\xi_{\mathrm{w}})=(1+\xi_{\mathrm{w}})^{3/10},\qquad s=(1+\xi_{\mathrm{w}})^{-3/10} \tag{20}$$

and the resultant single system for full numerical integration is

$$\begin{aligned}
&\frac{\partial^3\tilde{f}}{\partial\tilde{\eta}^3}+\frac{5+8\xi_{\mathrm{w}}}{5(1+\xi_{\mathrm{w}})}\tilde{f}\frac{\partial^2\tilde{f}}{\partial\tilde{\eta}^2}-\frac{6\xi_{\mathrm{w}}}{5(1+\xi_{\mathrm{w}})}\left(\frac{\partial\tilde{f}}{\partial\tilde{\eta}}\right)^2-5\left(\frac{\xi_{\mathrm{w}}}{1+\xi_{\mathrm{w}}}\right)^{3/2}\tilde{\theta}\\
&\quad=2\xi_{\mathrm{w}}\left\{\frac{\partial^2\tilde{f}}{\partial\tilde{\eta}\,\partial\xi_{\mathrm{w}}}\frac{\partial\tilde{f}}{\partial\tilde{\eta}}-\frac{\partial^2\tilde{f}}{\partial\tilde{\eta}^2}\frac{\partial\tilde{f}}{\partial\xi_{\mathrm{w}}}\right\},\\
&\frac{1}{\sigma}\frac{\partial^2\tilde{\theta}}{\partial\tilde{\eta}^2}+\frac{5+8\xi_{\mathrm{w}}}{5(1+\xi_{\mathrm{w}})}\tilde{f}\frac{\partial\tilde{\theta}}{\partial\tilde{\eta}}-\frac{(5+2\xi_{\mathrm{w}})}{5(1+\xi_{\mathrm{w}})}\tilde{\theta}\frac{\partial\tilde{f}}{\partial\tilde{\eta}}\\
&\quad=2\xi_{\mathrm{w}}\left\{\frac{\partial\tilde{f}}{\partial\tilde{\eta}}\frac{\partial\tilde{\theta}}{\partial\xi_{\mathrm{w}}}-\frac{\partial\tilde{f}}{\partial\xi_{\mathrm{w}}}\frac{\partial\tilde{\theta}}{\partial\tilde{\eta}}\right\}.
\end{aligned} \tag{21}$$

As $\tilde{\eta} \to \infty$

$$\frac{\partial \tilde{f}}{\partial \tilde{\eta}} = \frac{1}{(1+\xi_W)^{3/5}} \tag{22}$$

and again velocity profiles will evolve continuously between pure forced and pure free convection asymptotes.

4. Numerical Procedure

The numerical method employed was originally designed by Keller (Keller and Cebeci [5], Keller [6]) and has become known as the "Keller box" method.

Equations (12) and (21) are recast as a set of five simultaneous linear equations by introducing variables $\tilde{u}$, $\tilde{v}$, and $\tilde{w}$, they become

$$\frac{\partial \tilde{f}}{\partial \tilde{\eta}} = \tilde{u}, \tag{23a}$$

$$\frac{\partial \tilde{u}}{\partial \tilde{\eta}} = \tilde{v}, \tag{23b}$$

$$\frac{\partial \tilde{v}}{\partial \tilde{\eta}} + p_1(\xi)\tilde{f}\tilde{v} + p_2(\xi)\,\tilde{u}^2 + p_3(\xi)\tilde{\theta} = 2\xi\left\{\tilde{u}\frac{\partial \tilde{u}}{\partial \xi} - \tilde{v}\frac{\partial \tilde{f}}{\partial \xi}\right\}, \tag{23c}$$

$$\frac{\partial \tilde{\theta}}{\partial \tilde{\eta}} = \tilde{w}, \tag{23d}$$

$$\frac{1}{\sigma}\frac{\partial \tilde{w}}{\partial \tilde{\eta}} + p_1(\xi)\tilde{f}\tilde{w} + p_4(\xi)\,\tilde{\theta}\tilde{u} = 2\xi\left\{\tilde{u}\frac{\partial \tilde{\theta}}{\partial \xi} - \tilde{w}\frac{\partial \tilde{f}}{\partial \xi}\right\}, \tag{23e}$$

where for the uniform temperature case (a) $\xi = \xi_M$, $p_1 = 1 + \frac{1}{2}\chi$, $p_2 = -\chi$, $p_3 = 2\chi$ and $p_4 = 0$; and for the uniform heat flux case (b) $\xi = \xi_W$, $p_1 = 1 + \frac{3}{5}\chi$, $p_2 = -\frac{6}{5}\chi$, $p_3 = -5\chi^{3/2}$ and $p_4 = -(1 - \frac{3}{5}\chi)$ where in both cases $\chi = \xi/(1+\xi)$.

The boundary conditions (4) are

$$\begin{aligned} &\tilde{f} = \tilde{u} = 0, \quad \begin{cases} \text{(a)} & \tilde{\theta} = 1 \\ \text{(b)} & \tilde{w} = 1 \end{cases} && \text{on } \tilde{\eta} = 0 \\ &\begin{cases} \text{(a)} & \tilde{u} \to (1+\xi)^{-1/2}, \\ \text{(b)} & \tilde{u} \to (1+\xi)^{-3/5}, \end{cases} && \tilde{\theta} \to 0 \text{ as } \tilde{\eta} \to \infty. \end{aligned} \tag{24}$$

A net is placed on the $(\xi, \tilde{\eta})$ plane defined by

$$\begin{aligned} &\xi_0 = 0,\ \xi_n = \xi_{n-1} + k_n && n = 1, 2, \ldots, \\ &\tilde{\eta}_0 = 0,\ \tilde{\eta}_j = \tilde{\eta}_{j-1} + h_j && j = 1, 2, \ldots, N. \end{aligned} \tag{25}$$

TABLE I

g Sequences of $\tilde{v}$ at $\xi = 2$, $\tilde{\eta} = 0$ for (a) Uniform Temperature Case and (b) Uniform Heat Flux Case

(a)				
	1.106645			
	1.104518	1.103809	1.104038	
	1.104237	1.104012	1.104045	1.104046
	1.104150	1.104037		
(b)				
	1.909357			
	1.898554	1.894954	1.894514	
	1.896337	1.894563	1.894501	1.894501
	1.895541	1.894517		

Note. First column contains g_1, g_2, g_3 and g_4, second g_{12}, g_{23} and g_{34}, third g_{123} and g_{234} and fourth g_{1234}.

The values of ξ_n used are shown in Tables II and III and $\tilde{\eta}_j$ were taken as $\sinh(j/4)$ with $N = 12$ giving an outer boundary $\tilde{\eta}_N = 10.02$. If g_j^n denotes the value of any variable at $(\xi_n, \tilde{\eta}_j)$ then variables and derivatives of (23c), (23e) at $(\xi_{n-1/2}, \tilde{\eta}_{j-1/2})$ are replaced by

$$g_{j-1/2}^{n-1/2} = \tfrac{1}{4}(g_j^n + g_{j-1}^n + g_j^{n-1} + g_{j-1}^{n-1}),$$

$$\left(\frac{\partial g}{\partial \xi}\right)_{j-1/2}^{n-1/2} = \frac{1}{2k_n}(g_j^n + g_{j-1}^n - g_j^{n-1} - g_{j-1}^{n-1}),$$

$$\left(\frac{\partial g}{\partial \tilde{\eta}}\right)_{j-1/2}^{n-1/2} = \frac{1}{2h_j}(g_j^n + g_j^{n-1} - g_{j-1}^n - g_{j-1}^{n-1}),$$

where $\xi_{n-1/2} = \xi_{n-1} + \tfrac{1}{2}k_n$ and $\tilde{\eta}_{j-1/2} = \tilde{\eta}_{j-1} + \tfrac{1}{2}h_j$. Equations (23a), (23b), (23d), as they do not involve ξ explicitly, were centred at $(\xi_n, \tilde{\eta}_{j-1/2})$ using

$$g_{j-1/2}^n = \frac{1}{2}(g_j^n + g_{j-1}^n), \left(\frac{\partial g}{\partial \tilde{\eta}}\right)_{j-1/2}^n = \frac{1}{h_j}(g_j^n - g_{j-1}^n). \tag{26}$$

The boundary conditions (24) then imply

$$\tilde{f}_0^n = \tilde{u}_0^n = 0, \qquad \begin{matrix}(a)\ \tilde{\theta}_0^n = 1, \tilde{u}_N^n = (1+\xi_n)^{-1/2} \\ (b)\ \tilde{w}_0^n = 1, u_N^n = (1+\xi_n)^{-3/5},\end{matrix} \qquad \tilde{\theta}_N^n = 0.$$

If the problem has been solved up to ξ_{n-1} then we have $5N$ equations plus 5 boundary conditions for the $5N+5$ unknowns $(\tilde{f}_j^n, \tilde{u}_j^n, \tilde{v}_j^n, \tilde{\theta}_j^n, \tilde{w}_j^n)$, $j = 0, 1, \ldots, N$.

TABLE II

Flow Parameters for Uniform Temperature Case

ξ_M	$(\tilde{v})_0$	τ_w	$(\tilde{w}_0)$	Q
0.0	0.46960	∞	−0.46960	∞
0.2	0.66142	1.19905	−0.50547	0.83650
0.4	0.78117	1.12408	−0.52433	0.63766
0.6	0.86428	1.12242	−0.53611	0.55042
0.8	0.92556	1.13710	−0.54417	0.49830
1.0	0.97264	1.15668	−0.55000	0.46249
1.3	1.02581	1.18817	−0.55620	0.42479
1.6	1.06519	1.21922	−0.56051	0.39788
2.0	1.10406	1.25835	−0.56451	0.37147
2.5	1.13883	1.30325	−0.56784	0.34734
3.2	1.17224	1.35945	−0.57077	0.32299
4.0	1.19786	1.41609	−0.57279	0.30283
5.0	1.21935	1.47822	−0.57428	0.28422
7.0	1.24468	1.58239	−0.57568	0.25876
10.0	1.26375	1.70683	−0.57632	0.23469
15.0	1.27792	1.86652	−0.57630	0.21043
20.0	1.28439	1.99220	−0.57597	0.19495
30.0	1.28997	2.18789	−0.57526	0.17524
60.0	1.29359	2.57753	−0.57377	0.14638
100.0	1.29374	2.91456	−0.57267	0.12837
250.0	1.29207	3.64380	−0.57098	0.10164
10^3	1.28897	5.12925	−0.56922	0.07159
10^4	1.28599	9.09403	−0.56784	0.04015
10^6	1.28456	28.7236	−0.56721	0.01268
10^{10}	1.28439	287.199	−0.56715	0.00129
10^{16}	1.28439	9.08198×10^3	−0.56715	0.00004
10^{24}	1.28439	9.08198×10^6	−0.56715	0.00000

These are non-linear algebraic equations which are solved using Newton's iteration, the values of the variables at ξ^{n-1} being used as an initial iterate. At $\xi = 0$ Eqs. (23) only involve η explicitly and are discretized using (26), the resulting algebraic equations are again solved using Newton's iteration.

In order to employ Richardson's extrapolation each cell of the net (25) is divided into $2m$ subintervals[1] in the ξ direction and m subintervals in the $\tilde{\eta}$ direction, where m is an integer. The program was run for $m = 1, 2, 3$ and 4. If g_1, g_2, g_3 and g_4 are the results of a variable g at a given location $(\xi, \tilde{\eta})$ then the g_i have accuracy $O(h^2 + k^2)$,

[1] It was found that an odd number of subintervals tended to produce less accurate results. The division was always into equal subintervals except for the first step of case (b), where each subinterval is proportional to $\xi^{1/2}$. This was chosen because the expansion for small ξ is non-Maclaurin and depends on powers of $\xi^{3/2}$ (see Wilks [2]). The ensuing results were more accurate than when equal subintervals were used.

where $h = \max_j h_j$ and $k = \max_n k_n$. Since the truncation error is proportional to the square of h and k then

$$g_{12} = \tfrac{1}{3}(4g_2 - g_1), \qquad g_{23} = \tfrac{1}{5}(9g_3 - 4g_2), \qquad g_{34} = \tfrac{1}{7}(16g_4 - 9g_3)$$

have errors $O(h^4 + k^4)$ and

$$g_{123} = \tfrac{1}{8}(9g_{23} - g_{12}) \qquad \text{and} \qquad g_{234} = \tfrac{1}{3}(4g_{34} - g_{23})$$

will be in error by $O(h^6 + k^6)$ and finally

$$g_{1234} = \tfrac{1}{15}(16g_{234} - g_{123})$$

will have error $O(h^8 + k^8)$. Table I shows the g sequences for $\tilde{v}$ at $\xi = 2$, $\tilde{\eta} = 0$ illustrating the increases in accuracy that can be obtained. The results quoted are g_{1234} and the error is estimated by the difference $(g_{1234} - g_{234})$, which being a global error estimate measures the actual error in g. It should be appreciated that this error estimate is for g_{234} and hence we expect the results to be slightly more accurate than quoted later, say by perhaps one decimal place.

5. Numerical Results

In the first instance the "Keller box" method was used on the original transformed equations of Merkin and Wilks and entirely satisfactory agreement with their results was obtained. Once the basic program had been validated in this way, adaptation to the continuous transformation equations was readily achieved and the detailed numerical procedure of Section 4 was implemented.

The maximum estimated error difference $(g_{1234} - g_{234})$ over all variables is for the uniform temperature case (a) 3×10^{-6} and for the uniform heat flux case (b) 9×10^{-6}, we therefore anticipate the results to be accurate to 5 decimal places.

Figures 1 and 2 show the velocity profiles $\tilde{u}$ at various locations of ξ for (a) and (b), respectively, which are related to u by the formulae.

$$\text{(a)} \quad u = U(1 + \xi_M)^{1/2}\tilde{u} \qquad \text{(b)} \quad u = U(1 + \xi_W)^{3/5}\tilde{u}.$$

Tables II and III give the results for the skin friction coefficient defined by

$$\text{(a)} \quad \tau_w = \left(\frac{\nu}{Ug\beta[T_1 - T_0]}\right)^{1/2}\left(\frac{\partial u}{\partial y}\right)_0 = \frac{(1 + \xi_M)^{3/4}}{\sqrt{2\xi_M}}(\tilde{v})_0,$$

$$\text{(b)} \quad \tau_w = \left(\frac{5^2k^2\nu^2}{2^3U^4g^2\beta^2q^2}\right)^{1/6}\left(\frac{\partial u}{\partial y}\right)_0 = \frac{(1 + \xi_W)^{9/10}}{\sqrt{2\xi_W}}(\tilde{v})_0$$

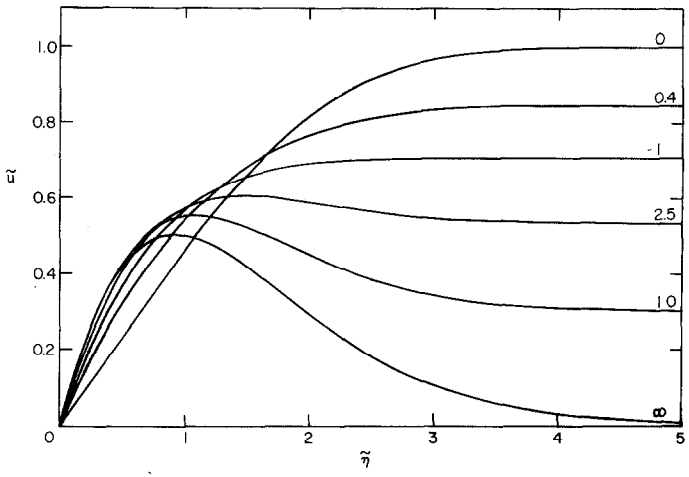

FIG. 1. Constant temperature velocity profiles. Numbers annotated to the profiles are ξ_M.

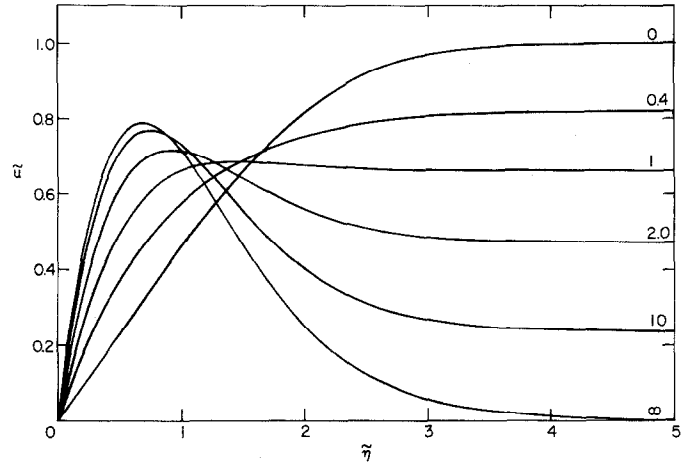

FIG. 2. Constant heat flux velocity profiles. Numbers annotated to the profiles are ξ_w.

and the heat transfer coefficient defined by

$$\text{(a)}\quad Q = -\left(\frac{vU}{g\beta[T_1 - T_0]}\right)^{1/2} \frac{1}{(T_1 - T_0)}\left(\frac{\partial T}{\partial y}\right)_0 = \frac{(1+\xi_M)^{1/4}}{\sqrt{2\xi_M}}(\tilde{w})_0,$$

$$\text{(b)}\quad Q = \left(\frac{5^2k^2v^2U^2}{2^3g^2\beta^2q^2}\right)^{1/6} \frac{1}{(T_{y=0} - T_0)}\left(\frac{\partial T}{\partial y}\right)_0 = -\frac{(1+\xi_w)^{3/10}}{\sqrt{2\xi_w}(\tilde{\theta})_0}.$$

The results are in good agreement with those of Merkin and Wilks. In view of the order of accuracy of the present algorithm compared to that used previously one would expect the present results to be the more accurate.

TABLE III

Flow Parameters for Constant Heat Flux Case

ξ_w	$(\bar{v})_0$	τ_w	$(\bar{\theta})_0$	Q
0.0	0.46960	∞	−1.54064	∞
0.1	0.56647	1.38011	−1.51405	1.15971
0.2	0.71201	1.32655	−1.46719	1.13825
0.4	0.97673	1.47824	−1.39585	0.88604
0.6	1.18675	1.65378	−1.34999	0.77860
0.8	1.35320	1.81571	−1.31881	0.71505
1.0	1.48753	1.96281	−1.29638	0.67152
1.3	1.64617	2.16045	−1.27259	0.62567
1.6	1.76876	2.33652	−1.25597	0.59284
2.0	1.89450	2.54609	−1.24037	0.56047
2.5	2.01166	2.77799	−1.22707	0.53072
3.2	2.12923	3.06236	−1.21489	0.50044
4.0	2.22363	3.34650	−1.20594	0.47514
5.0	2.30655	3.65847	−1.19872	0.45157
7.0	2.41075	4.18667	−1.19057	0.41890
10.0	2.49662	4.83160	−1.18479	0.38749
15.0	2.56883	5.68700	−1.18078	0.35523
20.0	2.60702	6.38427	−1.17911	0.33426
30.0	2.64685	7.51414	−1.17786	0.30707
60.0	2.68877	9.92566	−1.17746	0.26611
100.0	2.70636	12.1832	−1.17783	0.23972
250.0	2.72298	17.5900	−1.17886	0.19905
10^3	2.73202	30.6450	−1.18020	0.15054
10^4	2.73523	77.0049	−1.18126	0.09488
10^6	2.73575	485.918	−1.18165	0.03776
10^{10}	2.73579	1.93449×10^4	−1.18168	0.00598
10^{16}	2.73579	4.85923×10^6	−1.18168	0.00038
10^{24}	2.73579	7.70137×10^9	−1.18168	0.00001

6. Concluding Remarks

We have re-examined the computation of two members of the class of boundary layer flows displaying evolution between similarity regimes. When a prior knowledge of the final similarity regime is available it has been demonstrated that a continuous transformation may successfully be invoked which follows closely the natural evolution of the flow. Accordingly full numerical solution may be obtained in the context of a single transformed system of equations. When applied in conjunction with recent computational developments involving extrapolation on crude nets an efficient, accurate and straightforward algorithm ensues. The algorithm represents a significant improvement on those used previously and it therefore commends itself for general use in a wide class of boundary layer flows, including all such flows evolving from the general Falkner–Skan similairty states.

REFERENCES

1. J. H. MERKIN, *J. Fluid Mech.* **35** (1969), 439.
2. G. WILKS, *Int. J. Heat Mass Transfer* **17** (1974), 743.
3. S. OSTRACH, *NACA Ref.* **111** (1953).
4. E. M. SPARROW AND J. L. GREGG, *Trans. ASME* **78** (1956), 435.
5. H. B. KELLER AND T. CEBECI, Proc. Int. Conf. Numer. Meth. Fluid Dyn. 2nd, Berkeley, California (1971).
6. H. B. KELLER, *Ann. Rev. Fluid Mech.* **10** (1978), 417.